Time-Dependent Density Functional Theory As a Tool for Isomer Assignments of Hydrogen-Bonded Solute·Solvent Clusters

Markus Thut, Christian Tanner, Andreas Steinlin, and Samuel Leutwyler*

Departement für Chemie und Biochemie, Universität Bern, Freiestrasse 3, CH-3000 Bern 9, Switzerland

Received: January 25, 2008; Revised Manuscript Received: April 14, 2008

Can isomer structures of hydrogen-bonded solute·solvent clusters be assigned by correlating gas-phase experimental $S_0 \leftrightarrow S_1$ transitions with vertical or adiabatic excitation energies calculated by time-dependent density functional theory (TD-DFT)? We study this question for 7-hydroxyquinoline (7HQ), for which an experimental database of 19 complexes and clusters is available. The main advantage of the adiabatic TD-B3LYP $S_0 \leftrightarrow S_1$ excitations is the small absolute error compared to experiment, while for the calculated vertical excitations, the average offset is $+1810$ cm^{-1}. However, the empirically adjusted vertical excitations correlate more closely with the experimental transition energies, with a standard deviation of $\sigma = 72$ cm^{-1}. For the analogous correlation with calculated adiabatic TD-DFT excitations, the standard deviation is $\sigma = 157$ cm^{-1}. The vertical and adiabatic TD-DFT correlation methods are applied for the identification of isomers of the 7-hydroxyquinoline·$(MeOH)_n$, $n = 1-3$ clusters [Matsumoto, Y.; Ebata, T.; Mikami, N. *J. Phys. Chem. B* 2002, *106*, 5591]. These confirm that the vertical TD-DFT/experimental correlation yields more effective isomer assignments.

I. Introduction

When investigating the spectroscopic properties of molecular complexes and clusters in supersonic molecular jet expansions, the assignment of the experimental electronic spectra to specific cluster isomers has emerged as a challenging task.[1–17] Recently, we have explored the possibility of assigning the isomer structures of hydrogen-bonded solute·solvent clusters by correlating the observed origins of the $S_0 \leftrightarrow S_1$ transitions with the vertical excitation energies calculated by time-dependent density functional theory (TD-DFT).[18–21]

A large number of density functional theory (DFT) studies have treated excited-state properties based on the time-dependent (TD) propagator method. Most of these employ the geometric structure of the electronic ground state, yielding *vertical* excitation energies and oscillator strengths. More recently, excited-state analytical gradients have been implemented for propagator methods.[22–24] So far, however, relatively few studies have addressed the calculation of adiabatic excitation energies; Furche et al. and Rappoport et al. have calculated adiabatic excitation energies and S_1 relaxed structures by TD-DFT, comparing the ab initio calculated values to experiment for various functionals.[22,25] Excited-state geometry optimizations, potential energy surface scans, and reaction pathways have been explored using TD-DFT for individual molecules[26–31] and also for several hydrogen-bonded complexes and clusters.[32–36] Further work was done for excited-state optimizations using TD-DFT with long-range corrected functionals.[37] The results were compared to the experimental and adiabatic excitation energies already computed by Furche et al.[22]

TD-DFT computational studies of the solvatochromic shifts of substituted coumarins in bulk solution were performed by Jacquemin et al.[38] and Preat et al.,[39] who treated the solvation effects with the PCM model.[40] TD-DFT excitation energy calculations of the solvatochromic effects of acetone in different sized solvent shells were performed using the frozen density embedding scheme, which allows explicit treatment of the solvent molecules.[41] The microsolvation effects of van der Waals interactions between rare-gas atoms and the π-electron cloud of arenes as well as O−H···π-electron H-bond interactions have been treated at the CASSCF level.[42]

So far, no comparison of the computed vertical and adiabatic excitation energies for a series of structurally related molecular clusters has been reported. Over the last years, we have measured a series of electronic spectra of supersonic jet-cooled 7-hydroxyquinoline and 7-hydroxyquinoline·solvent clusters. By correlating the experimental with the calculated vertical TD-B3LYP excitation energies, we have been successful in assigning several cluster isomer structures to the observed $S_0 \rightarrow S_1$ origins.[19–21] The 7-hydroxyquinoline (7HQ) aromatic molecule offers a "strong" O−H and a "weak" C−H hydrogen-bond donor site and a single H-bond-acceptor site (quinolyl-N). In combination with the two possible rotamers at the −O−H group, this yields a potentially large array of possible H-bonded species. Specifically, we have calculated the vertical TD-B3LYP excitations for bare *cis*- and *trans*-7-hydroxyquinoline,[43] the *cis*-7HQ·$(H_2O)_n$, $n = 1-3$ and *trans*-7HQ·H_2O clusters,[43–45] the *cis*-7HQ·$(NH_3)_n$, $n = 1-3$ and *trans*-7HQ·NH_3 clusters,[46–48] the mixed solvent clusters of *cis*-7HQ·$(NH_3)_n$·$(H_2O)_m$, $n + m = 3$, $n, m \geq 1$,[20,21] and the two isomers of the *cis*-7HQ·HCOOH complex.[49] A selection of above-quoted cluster structures is displayed in Figure 1. So far, these investigations have shown excellent correlations between experiment and calculated vertical excitation energies.

Below, we explore the correlation of TD-DFT calculated vertical and adiabatic $S_0 \rightarrow S_1$ excitations with the respective experimental values. Secondly, we investigate the relative performance of both techniques for the assignment of cluster isomers. Finally, we present an application of isomer assignments to the series of 7HQ·(methanol)$_n$ clusters.[13,43]

* To whom correspondence should be addressed.

10.1021/jp801044x CCC: $40.75
Published on Web 05/30/2008

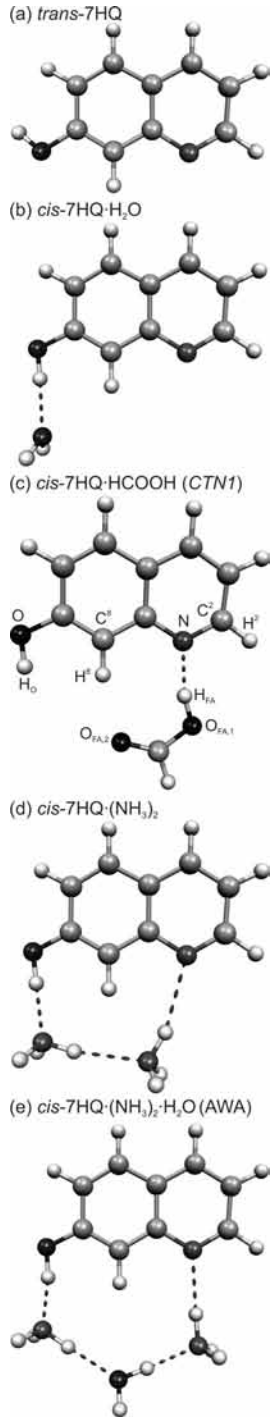

Figure 1. Selected structures of clusters of 7-hydroxyquinoline (7HQ): (a) *trans*-7HQ, (b) *cis*-7HQ·H_2O, (c) *cis*-7HQ·HCOOH (CTN1) with atom labeling, (d) *cis*-7HQ·$(NH_3)_2$, and (e) *cis*-7HQ·$(NH_3)_2$·H_2O (AWA).

II. Theoretical Methods

The 6-311++G(d,p) basis set was used for S_0 and S_1 state calculations of all complexes and clusters. The ground-state structures were optimized with the B3LYP hybrid density functional[50] using a pruned (99,590) grid for numerical integration and were optimized until the forces were $<2 \times 10^{-6}$ hartree/bohr or hartree/rad. Very tight SCF convergence criteria of RMS density matrix element differences $< 10^{-9}$ were applied.

The vertical $S_0 \leftrightarrow S_1$ excitation energies were calculated with the time-dependent DFT method using the B3LYP functional (TD-B3LYP), at the B3LYP-optimized S_0 state structures, using Gaussian03.[40] For the adiabatic excitation energies, we optimized both the S_0 and S_1 geometries with the B3LYP method implemented in TURBOMOLE 5.9.[23] The difference of the optimized S_0 and the corresponding S_1 minimum energies was taken as the adiabatic excitation energy. Note that the B3LYP density functional in TURBOMOLE and Gaussian03 differ in the formulation of the local density approximation (LDA) part. Vosko et al. proposed various fitting schemes for the LDA functional,[51] and the VWN(V) scheme is implemented in TURBOMOLE,[23] while the VWN(III) scheme is implemented in Gaussian03.[22,40] However, the influence of the different implementations of the B3LYP functional on the relative S_0 energies was found to be small.

III. Results

A. Vertical TD-B3LYP Excitations. The TD-B3LYP-calculated $S_0 \rightarrow S_1$ vertical excitation energies of the 7HQ complexes and clusters are compared to the experimental electronic origins in Table 1. The calculated vertical excitations all lie above the observed 0_0^0 bands, with an average offset $\bar{\Delta} = [\sum_i^n (E_{calc} - E_{exp})]/n$ of $+1810$ cm^{-1} relative to the experiment. As will be seen below, the calculated adiabatic energies are rather close to experiment. Thus, the positive offset is not due to errors of the TD-B3LYP calculation but (to a large part) reflects the fact that vertical excitation energies from S_0-optimized structures should lie higher than the experimental origins, which correspond to adiabatic excitations.

Apart from the overall offset, the calculated vertical excitation energies are somewhat too high for the bare 7HQ and the 7HQ·solvent complexes and too low for clusters ($n \geq 2$); see Table 1. The excited-state relaxation energy, that is, the calculated vertical minus adiabatic excitation energy of the chromophore, can be assumed to be approximately constant. In this approximation, the remaining relaxation energy depends on the impact of the $\pi\pi^*$ excitation on the hydrogen-bond interactions. This contribution increases with increasing cluster size, which justifies the use of a nonlinear fit curve.[21] A quadratic polynomial was fitted to the calculated/experimental data points. All values lie within the 2σ interval, and 13 out of 15 values lie within the 1σ interval; see Figure 2. The largest residuals Δ (=fitted transition energy minus calculated transition energy) are < 160 cm^{-1}. The Δ residuals and goodness-of-fit parameters are given in Table 1.

B. Adiabatic TD-B3LYP Excitations. To compare with the vertical $S_0 \rightarrow S_1$ transition energies, we calculated the adiabatic transitions for all monomers and clusters mentioned above; these are also compiled in Table 1. The adiabatic excitation energies exhibit an average offset of only $+180$ cm^{-1} relative to experiment. This shows that the good performance of the time-dependent B3LYP method[22,25] extends also to H-bonded complexes and clusters. The lowering of the adiabatic transitions relative to the vertical values is of course expected.

The origins of the bare *cis*- and *trans*-7HQ rotamers are calculated to be 405 and 128 cm^{-1} above the respective experimental values. For the complexes, the adiabatic calculations are very close to experiment; for example, the *cis*-7HQ·NH_3, *cis*-7HQ·H_2O, and *trans*-7HQ·H_2O adiabatic excitation energies are only $+13$, $+2$, and -114 cm^{-1} off of the experimental values, respectively. The formic acid isomer *cis*-7HQ·HCOOH (CTN2) is also predicted to be very close to experiment ($+58$ cm^{-1}). In contrast, the adiabatic excitations of the *cis*-7HQ·HCOOH CTN1 isomer, of *trans*-7HQ·NH_3, and of the clusters are generally predicted to be too low with respect to experiment.

TABLE 1: Experimental $S_0 \rightarrow S_1$ Excitation Energies, TD-B3LYP-Computed Vertical and Adiabatic Excitation Energies, and Fit Residuals Δ (fitted − calculated value), in cm^{-1}

cluster	experimental	vertical	Δ	adiabatic	Δ
cis-7HQ	30830	33024	−46	31235	−37
cis-7HQ·HCOOH (CTN2)	30657	32649	49	30715	162
cis-7HQ·H_2O (O−H···O)	30240	32110	−33	30253	−89
cis-7HQ·NH_3	29925	31786	−128	29927	−246
cis-7HQ·HCOOH (CTN1)	29816	31579	−56	29391	134
cis-7HQ·$(H_2O)_2$	29193	30808	44	28612	133
cis-7HQ·$(NH_3)_2$	29115	30785	−5	28738	−78
cis-7HQ·$(NH_3)_3$ (3ch3)	28800	30569	−53	28450	−100
cis-7HQ·$(H_2O)_3$ (3ch3)	28770	30469	24	27980	342
cis-7HQ·$(NH_3)_2$·H_2O (AWA)	28694	30437	0	28355	−99
cis-7HQ·$(NH_3)_2$·H_2O (AAW)	28348	30260	−47	28075	−87
cis-7HQ·$(H_2O)_2$·NH_3 (AWW)	28340	30157	51	27998	−16
trans-7HQ	30551	32483	50	30679	9
trans-7HQ·H_2O (O−H···O)	29995	31755	−7	29881	−97
trans-7HQ·NH_3	29792	31337	157	29428	64
R^2 of quadratic fit		0.9949		0.9822	
standard deviation σ		72.2		157.2	

We performed a quadratic fit through the obtained data points as for the vertical $S_0 \rightarrow S_1$ transitions and found all values within the 2σ interval. Twelve out of 15 predictions lie within the 1σ interval of the quadratic fit polynomial; see Figure 3. The largest residuals are $< 350\ cm^{-1}$. The Δ residuals and goodness-of-fit parameters are also given in Table 1.

C. Electronic Transitions of the 7-Hydroxyquinoline·(Methanol)$_n$, $n = 1-3$, Clusters. Here, we discuss the application of the vertical and adiabatic TD-B3LYP methods as diagnostic tools for the isomer identification of the analogous 7-hydroxyquinoline/methanol clusters, that is, 7HQ·$(MeOH)_n$, $n = 1-3$. The $S_0 \leftrightarrow S_1$ transitions of two isomers of 7-hydroxyquinoline·MeOH were measured by Lahmani et al.[43] Later, Matsumoto et al.[13] measured laser-induced fluorescence excitation (LIF), fluorescence emission, UV−UV holeburning, and fluorescence-dip infrared (FDIR) spectra of the 7HQ·$(MeOH)_n$, $n = 1-3$, clusters. They assigned the isomers and interpreted the FDIR spectra based on B3LYP/6-31G(d,p)-calculated infrared spectra. They also reported spectral features of clusters larger than $n = 3$.

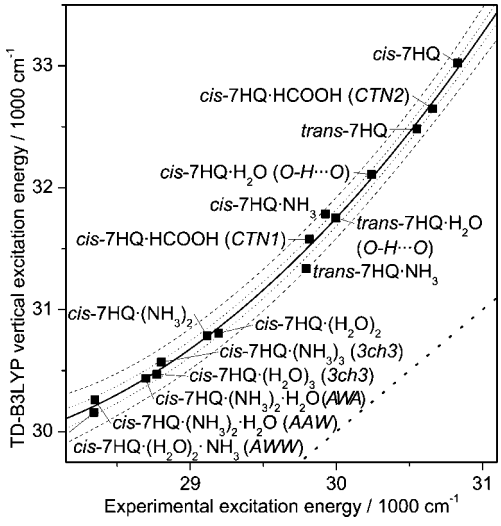

Figure 2. Calculated vertical TD-B3LYP $S_0 \rightarrow S_1$ excitation energies of 7-hydroxyquinoline·(solvent)$_n$, $n = 1-3$, clusters with different hydrogen-bonded solvent molecules versus the experimental 0_0^0 transition energies (■). Data points were fitted with a quadratic polynomial (full line). The 95 (dashed) and 60% (dotted) confidence interval bands are also displayed. The dotted diagonal line indicates ideal agreement between theory and experiment.

For the 7HQ·MeOH complex, both groups noted two isomers (denoted A and B, respectively) with LIF spectra of roughly equal intensity and origin transitions lying at 30131 (A) and 30363 cm^{-1} (B). Lahmani et al. assigned these spectra as the trans and cis rotamers of the complex with the 7HQ hydroxy group bonded to the MeOH acting as the acceptor (O−H···O isomer).[43] In contrast, Matsumoto et al. assigned both species to the cis rotamer of 7HQ, band A to the *cis*−O−H···O isomer, and band B to the *cis*−N···H−O isomer, with MeOH acting as a H donor to the quinolyl-N acceptor site.[13] The latter reassignment was based on analogy to the spectral shifts observed for the H_2O and NH_3 complexes and on the comparison of the FDIR spectra of the A and B species to B3LYP/6-31G(d,p)-scaled vibrational frequencies.[13] While the agreement of calculated and FDIR spectra is excellent for isomer B,[13] it is not as good for isomer A, casting some doubt on this assignment. Also, Matsumoto et al. did not calculate the IR spectra for the putative *trans*−O−H···O and *trans*−N···H−O isomers, leaving the comparison incomplete.

Due to the structural similarity of the 7HQ/methanol clusters to the 7HQ/water and 7HQ/ammonia clusters, and since there are conflicting assignments for the $n = 1$ complex, an investigation of the 7HQ/methanol clusters seemed appropriate as a test for the TD-B3LYP method. We optimized the structures with the same procedure and convergence criteria as above. For 7HQ·MeOH, four possible isomers were considered, that is, the O−H···O and N···H−O isomers for both rotamers of 7HQ. For the *cis*-7HQ·$(MeOH)_n$ ($n = 2, 3$) clusters, the solvent-wire isomers are calculated to be the most stable. The next higher-energy isomers have cyclic (ring) H-bonding geometries involving the 7HQ −O−H group as both the H donor and acceptor and lie higher by 3.1 and 5.1 kcal/mol, respectively. The optimized ground-state structures are shown in Figure 4. The calculated vertical and adiabatic $S_0 \rightarrow S_1$ transition energies and experimental electronic origins[13] are given in Table 1 and are plotted in Figures 4 and 5.

For 7HQ·MeOH, the vertical/experimental correlation in Figure 5 predicts that the "A" origin at 30131 cm^{-1} and the "B" frequency origin at 30363 cm^{-1} are due to the *cis*-7HQ·MeOH (O−H···O) and (N···H−O) isomers, respectively. This assignment is in agreement with that given by Matsumoto et al.[13] Both data points lie within the 60% confidence interval of the fit function. The only other point within the 95% confidence band is due to the *trans*-7HQ·MeOH (N···H−O) isomer; see Figure 5. Assignments to the *trans*-

TABLE 2: B3LYP/6-311++G(d,p)-Computed Properties for the 7-Hydroxyquinoline·(MeOH)$_n$, $n = 1-3$, Clusters[a]

cluster	E_{rel}	experimental[b]	vertical	Δ	adiabatic	Δ
cis-7HQ·MeOH (N···*H*O)	0.33[c]	30363	32186	67	30184	182
cis-7HQ·MeOH (OH···O)	0.00[c]	30131	31994	−67	30149	−158
trans-7HQ·MeOH (N···HO)	2.39[c]		31831	96	29797	194
trans-7HQ·MeOH (OH···O)	1.02[c]		31641	287	29778	213
cis-7HQ·(MeOH)$_2$ (2ch2)	0.00[d]	28962	30730	−83	28530	−27
cis-7HQ·(MeOH)$_2$ (2cy2)	3.13[d]		32464	−1818	*f*	
cis-7HQ·(MeOH)$_3$ (3ch3)	0.00[e]	28501	30292	13	28188	−89
cis-7HQ·(MeOH)$_3$ (3cy3)	5.14[e]		32497	−2191	30502	−2403

[a] Relative energies E_{rel} in kcal/mol and experimental, vertical, and adiabatic $S_0 \rightarrow S_1$ transitions and fit residuals Δ in cm^{-1}. [b] Ref 13. [c] Relative to the total energy of *cis*-7HQ·MeOH (OH···O), −592.7104349 au. [d] Relative to the total energy of *cis*-7HQ·(MeOH)$_2$ (2ch2), −708.4285914 au. [e] Relative to the total energy of *cis*-7HQ·(MeOH)$_3$ (3ch3), −824.1507593 au. [f] Minimizes to the (2ch2) structure in the S_1 state.

7HQ·MeOH (O−H···O) isomer can be ruled out based on the correlation. The *cis*-7HQ·(MeOH)$_2$ (2ch2) and *cis*-7HQ·(MeOH)$_3$ (3ch3) clusters are nicely predicted by the interpolating curve, the first within the 95% and the latter within the 60% prediction band. The corresponding two cyclic isomers (2cy2) and (3cy3) are strongly blue shifted by about 1820 and 2200 cm^{-1}, respectively, and are thus ruled out.

The adiabatic excitation energies in Figure 6 lie very close for the 7HQ·MeOH (O−H···O) and (N···H−O) isomers. Of the four possibilities, the higher-lying experimental electronic origin (30363 cm^{-1}) is closest to the predicted *cis*-7HQ·MeOH (N···H−O) isomer. However, the value is outside of the 60% confidence interval, and the predicted frequency of the corresponding O−H···O isomer also lies within the 95% prediction band. The assignment of the red-shifted electronic origin (30131 cm^{-1}) is even more delicate; here, all four calculated transition energies lie outside of the 60 and within the 95% confidence interval. The closest-lying point is that of the *cis*-7HQ·MeOH (O−H···O) isomer, but a determination of the isomer based only on the adiabatic excitation energy alone would be ambiguous. Consideration of the relative total energies of the isomers (Table 1, second column) also points to the *cis*-7HQ·MeOH (O−H···O) isomer. The energy of the corresponding *trans*-7HQ·MeOH (O−H···O) isomer is ∼1 kcal/mol higher, and that of the *trans*-7HQ·MeOH (N···H−O) isomer is 2.4 kcal/mol higher.

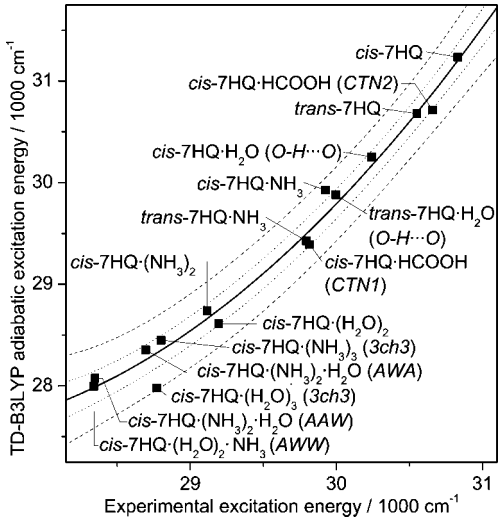

Figure 3. Calculated adiabatic TD-B3LYP $S_0 \rightarrow S_1$ excitation energies of 7-hydroxyquinoline·(solvent)$_n$, $n = 1-3$, clusters with different hydrogen-bonded solvent molecules versu the experimental 0_0^0 transition energies (■). Fit and confidence interval bands as those in Figure 2.

In contrast, the *cis*-7HQ·(MeOH)$_n$ ($n = 2, 3$) solvent-wire clusters show very good agreement based on their predicted adiabatic transition energies and lie within the 60% prediction limit (see Figure 6). The corresponding cyclic (3cy3) cluster exhibits a blue shift comparable to that predicted for the vertical excitation. For the (2cy2) cluster, structure optimization leads to the (2ch2) isomer, and no adiabatic excitation energy could be determined.

The assignment of cluster structures based on the excitation energies relies on the comparison of a single number. In all cases investigated so far, the assignment of isomer structures has been in agreement with the B3LYP-calculated relative cluster energy E_{rel}, that is, the total energy of a cluster isomer relative to the most stable isomer. Being a property of the cluster ground state only, these represent an independent set of data that can be used to corroborate the calculated excitation energies.

IV. Discussion

If we disregard the overall offset between the calculated and experimental transition energies, the vertical TD-B3LYP calculations yield higher-precision predictions. The calculated 0_0^0 transitions all lie within ±160 cm^{-1} of the quadratic fit polynomial, and the vertical TD-B3LYP fit (Figure 2) has a standard deviation of $\sigma = 72$ cm^{-1}. As the assignment of the 7-hydroxyquinoline·(MeOH)$_n$ clusters shows, the use of the calculated vertical excitations yields reliable results. If the electronic transitions of different isomers are predicted to lie close in energy or if the experimental close-lying $S_0 \rightarrow S_1$ origins are close, clear discrimination between different isomer geometries can be difficult. The major drawback of the vertical excitation energies is that an empirically adjusted energy shift is needed; when new molecular systems are considered, such a fit may be impossible or inaccurate.

The remarkable advantage of the computed adiabatic excitation energies is their small absolute errors, which do not necessitate any additional fitting of the energy shift (as for the vertical excitation energies). On the other hand, the adiabatic excitation energy predictions are somewhat less reliable. The standard deviation of the fit for the adiabatic calculations is $\sigma = 157$ cm^{-1}, about twice that of the vertical calculations. This is also seen when comparing the confidence interval bands of Figure 3 with respect to those of Figure 2. Another drawback of the adiabatic calculations is that the computational time is up to 50× larger.

The somewhat larger standard deviation of the adiabatic relative to the vertical excitation energies should not be overemphasized. Firstly, it could be due to zero-point vibrational energy (ZPVE) differences that are contained in the experimental

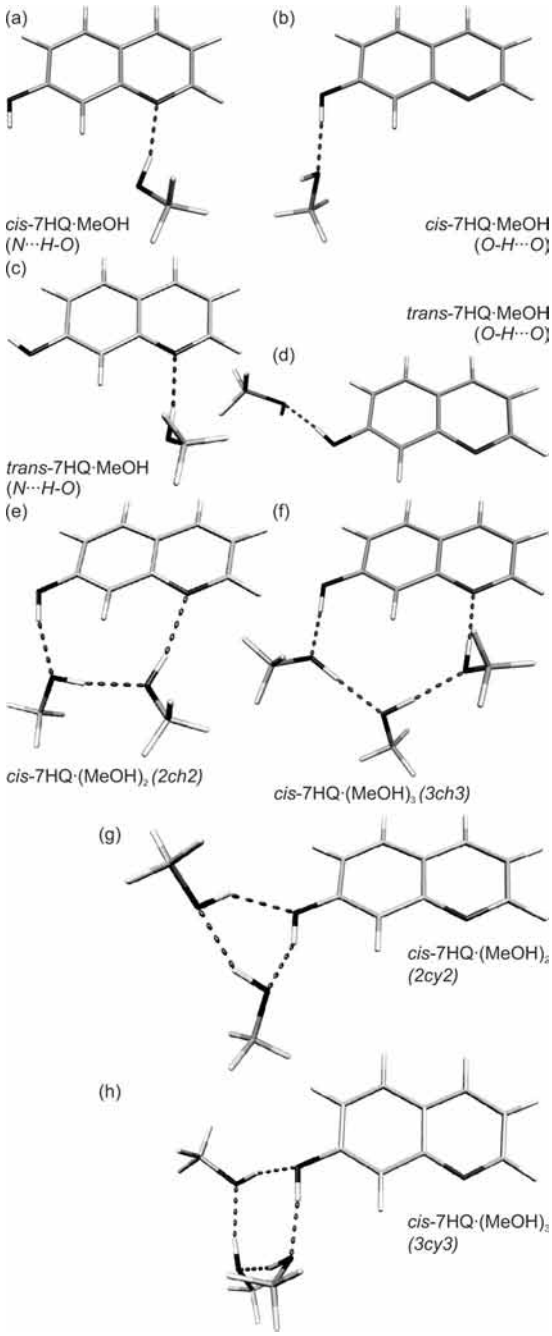

Figure 4. B3LYP/6-311++G(d,p)-optimized S_0 state structures of (a, b) *cis*-7-hydroxyquinoline·MeOH complexes with the methanol bound to the hydroxy group or the quinolyl-N, (c, d) the analogous *trans*-7-hydroxyquinoline·MeOH complexes, (e) *cis*-7-hydroxyquinoline·$(MeOH)_2$ (2ch2) cluster, (f) *cis*-7-hydroxyquinoline·$(MeOH)_3$ (3ch3) wire cluster, and (g, h) the corresponding (2cy2) and (3cy3) cyclic clusters, respectively.

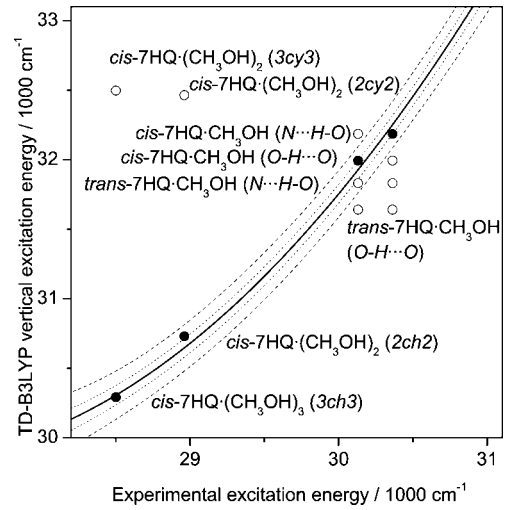

Figure 5. Calculated vertical TD-B3LYP $S_0 \rightarrow S_1$ transitions of 7HQ·$(MeOH)_n$ clusters versus the experimental 0_0^0 transitions, taken from ref 13. The assigned isomers are marked by •, and alternative correlations are marked by ○. The calibration curve and confidence intervals are those of Figure 2.

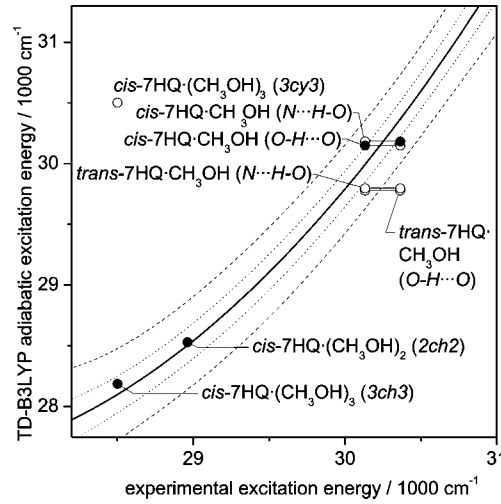

Figure 6. Calculated adiabatic TD-B3LYP $S_0 \rightarrow S_1$ transitions of 7HQ·$(MeOH)_n$ clusters versus the experimental 0_0^0 transitions, taken from ref 13. The assigned isomers are marked by •, and alternative correlations are marked by ○. The calibration curve and confidence intervals are those of Figure 3.

adiabatic excitation energies but are not included in the calculation (the calculation of S_1 state vibrational frequencies can currently only be done numerically, at prohibitive computational cost). Secondly, basis set effects (e.g., inclusion of *f* polarization functions) might affect the results. Nevertheless, we have explored two possible problem areas of the TD-B3LYP calculations:

(1) The calculated vertical excitation energies are influenced by (i) the quality of the B3LYP description of the S_0 state electronic wave function, (ii) the limitations of the linear response ansatz in describing the S_1 excited state potential, and (iii) the B3LYP description of the hydrogen-bond interactions in the S_0 and S_1 states at the S_0 state geometry. The adiabatic excitation energies additionally depend on the accuracy of the TD-B3LYP description of the S_1 state cluster equilibrium structures. We considered the possibility that the larger variance exhibited by the adiabatic calculations is due to problems with the TD-B3LYP S_1 state cluster geometries. To diagnose this, we searched for correlations of large Δ values with unusual H-bond geometry changes. The calculated heavy-atom hydrogen-bond distances between the 7HQ moiety and the solvent molecule(s) are listed in Table 3, together with the TD-B3LYP-calculated changes in H-bond length that occur upon $S_0 \rightarrow S_1$ electronic excitation. Large changes on the order of ± 0.2 Å are predicted for the 7HQ·HCOOH isomers CTN1 and CTN2, specifically for the weak C−H···O=C hydrogen bonds between 7HQ and the C=O group of the HCOOH moiety. However, while the CTN1 and CTN2 isomers show considerable ΔR values, they are not the largest outliers in Figure 3. A large change of H-bond distance is predicted for the long (and weak) N−H···N hydrogen bond from the second NH_3 moiety of *cis*-

TABLE 3: Calculated Heavy-Atom Distances (in Å) of the Hydrogen Bond(s) Linking 7-Hydroxyquinoline to the Solvent Molecules[a]

cluster	sistance R^b	S_0 state	S_1 state	ΔR ($S_1 - S_0$)
cis-7HQ·HCOOH (CTN2)	$R(N_Q\cdots O_H)$	2.7134	2.6460	−0.0674
	$R(C^2\cdots O{=}C)$	3.3190	3.5247	0.2056
cis-7HQ·H_2O (O−H···*O*)	R(O···O)	2.8288	2.7555	−0.0733
cis-7HQ·NH_3	R(O···N)	2.8348	2.7442	−0.0906
cis-7HQ·HCOOH (CTN1)	$R(N_Q\cdots O_H)$	2.7263	2.6241	−0.1022
	$R(C^8\cdots O{=}C)$	3.3020	3.1078	−0.1942
cis-7HQ·$(H_2O)_2$	R(O···O)	2.9247	2.7588	−0.1659
	$R(N_Q\cdots O)$	2.9530	2.8010	−0.1520
cis-7HQ · $(NH_3)_2$	R(O···N)	2.8339	2.7157	−0.1182
	$R(N_Q\cdots N)$	3.4209	3.2324	−0.1885
cis-7HQ·$(NH_3)_3$ (3ch3)	R(O···N)	2.7432	2.6159	−0.1272
	$R(N_Q\cdots N)$	3.1814	3.0867	−0.0947
cis-7HQ·$(H_2O)_3$ (3ch3)	R(O···O)	2.7205	2.6052	−0.1153
	$R(N_Q\cdots O)$	2.7857	2.6964	−0.0893
cis-7HQ·$(NH_3)_2$·H_2O (AWA)	R(O···N)	2.7434	2.6147	−0.1287
	$R(N_Q\cdots N)$	3.1244	3.0244	−0.1000
cis-7HQ·$(NH_3)_2$·H_2O (AAW)	R(O···N)	2.7400	2.6047	−0.1353
	$R(N_Q\cdots O)$	2.8264	2.7383	−0.0881
cis-7HQ·$(H_2O)_2$·NH_3 (AWW)	R(O···N)	2.7423	2.6075	−0.1347
	$R(N_Q\cdots O)$	2.7867	2.6983	−0.0884
trans-7HQ·H_2O (O−H···O)	R(O···O)	2.8414	2.8388	−0.0026
cis-7HQ·MeOH (OH···O)	R(O···O)	2.7884	2.7097	−0.0787
cis-7HQ·MeOH (N···HO)	$R(N_Q\cdots O)$	2.8965	2.8096	−0.0869
cis-7HQ·$(MeOH)_2$ (2ch2)	R(O···O)	2.8667	2.7112	−0.1555
	$R(N_Q\cdots O)$	2.9863	2.8200	−0.1663
cis-7HQ·$(MeOH)_3$ (3ch3)	R(O···O)	2.6871	2.5711	−0.1160
	R(N···O)	2.7980	2.7072	−0.0908

[a] B3LYP or TD-B3LYP methods with the 6-311++G(d,p) basis set. [b] N_Q: quinolyl-N of 7HQ; O=C and OH refer to HCOOH. For atom labeling, please refer to Figure 1c.

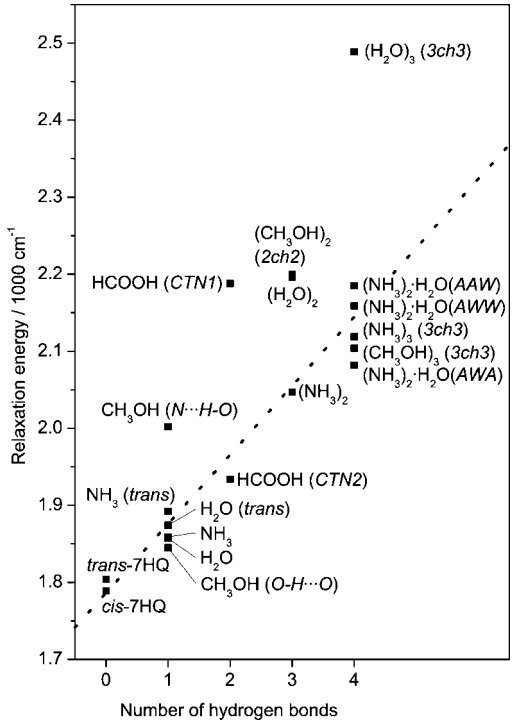

Figure 7. Calculated TD-B3LYP S_1 state relaxation energies for the 7-hydroxyquinoline·(solvent)$_n$ clusters as a function of the number of hydrogen bonds. Values referring to the *trans*-7-hydroxyquinoline rotamer are noted explicitly; all others refer to the *cis* rotamer. See text for details.

7HQ·$(NH_3)_2$ to the quinolyl-N. However, the adiabatic transition energy of *cis*-7HQ·$(NH_3)_2$ lies close to the fit parabola. The largest outlier in Figure 3 is the adiabatic transition energy for the *cis*-7HQ·$(H_2O)_3$ cluster, lying 342 cm^{-1} below the fit. For this cluster, however, the calculated geometry changes are in line with the H-bond geometries of the *cis*-7HQ·H_2O and *cis*-7HQ·$(H_2O)_2$ clusters. We conclude that the larger variance exhibited by the adiabatic/experimental correlation is not due to problems of TD-B3LYP in describing the solute−solvent hydrogen bonds in the S_1 state.

(2) An alternative is that the larger deviations of the adiabatic/experimental correlation arise for clusters that undergo large S_1 state relaxation between the vertical Franck−Condon point and the S_1 state minimum energy. Figure 7 shows the TD-B3LYP-calculated S_1 state relaxation energies. An intramolecular relaxation energy of ∼1800 cm^{-1} is associated with the 7-hydroxyquinoline chromophore, both for the cis and trans forms. The diagonal dotted line indicates that for 12 of the 17 clusters, the relaxation energy increases roughly linearly with the number of hydrogen bonds in the cluster, in agreement with the argument given at the end of section III.A. Significantly, Figure 7 shows that, with the exception of the *cis*-7HQ·HCOOH (CTN2) isomer, all clusters that involve a O−H group as a proton donor to the quinolyl-N undergo a relaxation in the S_1 state that is 100−350 cm^{-1} larger than that calculated for the other clusters. Comparison of Figure 7 with Figures 3 and 6 shows that these are also the complexes or clusters that show the largest deviations from the adiabatic fit curve. We conclude that the slightly larger deviations from the adiabatic/experimental correlation curve (compared to the vertical/experimental correlation) may arise from the TD-B3LYP-calculated relaxation associated with the O−H···N hydrogen bond to the quinolyl-N group.

V. Conclusions

For a series of 19 hydrogen-bonded complexes and clusters involving 7-hydroxyquinoline, we have investigated the cor-

relation of the calculated TD-B3LYP $S_0 \rightarrow S_1$ vertical and adiabatic excitation energies with the experimental electronic origins as a tool for isomer identification and structure assignment.

The TD-B3LYP-computed adiabatic excitation energies are close to the experimental excitation energies in absolute terms, typically within 400 cm^{-1}. This small absolute error is truly remarkable and shows that the good performance of the time-dependent B3LYP method[22,25] extends also to H-bonded complexes and clusters. The computed vertical excitation energies are shifted about 1800 cm^{-1} higher than the experimental values but yield even smaller standard deviations from the shifted mean than the adiabatic ones.

We have studied the consequences of the $\pi\pi^*$ electronic excitation in the 7HQ chromophore on (i) specific hydrogen bonds between 7HQ and the solvent molecule(s) and (ii) the S_1 state relaxation energies. The analysis indicates that the somewhat larger deviation of the adiabatic/experimental correlation (relative to the vertical/experimental correlation) can be traced to the relatively large relaxation energies predicted for clusters that involve a O−H group as the proton donor to the quinolyl-N. However, it is not possible to attribute the extent of relaxation to specific geometry changes within the cluster.

In summary, the identification of different structural isomers based on the correlation of TD-B3LYP vertical excitations with experiment is slightly better than that when using the calculated adiabatic excitations. These investigations are currently being extended to structurally related clusters.[52]

Acknowledgment. This work was supported by the Schweiz. Nationalfonds (Project 200020−113798).

References and Notes

(1) Troxler, T.; Knochenmuss, R.; Leutwyler, S. *Chem. Phys. Lett.* **1989**, *159*, 554.
(2) Bösiger, J.; Bombach, R.; Leutwyler, S. *J. Chem. Phys.* **1991**, *94*, 5098.
(3) Bieske, E. J.; Uichanco, A. S.; Rainbird, M. W.; Knight, A. E. W. *J. Chem. Phys.* **1991**, *94*, 7029.
(4) Troxler, T.; Leutwyler, S. *J. Chem. Phys.* **1991**, *95*, 4010.
(5) Troxler, T.; Stratton, J. R.; Smith, P. G.; Topp, M. R. *Chem. Phys. Lett.* **1994**, *222*, 250.
(6) Ishikawa, S.; Ebata, T.; Ishikawa, H.; Inoue, T.; Mikami, N. *J. Phys. Chem.* **1996**, *100*, 10531.
(7) Janzen, C.; Spangenberg, D.; Roth, W.; Kleinermanns, K. *J. Chem. Phys.* **1999**, *110*, 9898.
(8) Spangenberg, D.; Imhof, P.; Roth, W.; Kleinermanns, K. *J. Phys. Chem. A* **1999**, *103*, 5918.
(9) Carney, J. R.; Zwier, T. S. *J. Phys. Chem. A* **1999**, *103*, 9943.
(10) Fernandez, J. A.; Longarte, A.; Unamuno, I.; Castano, F. *J. Chem. Phys* **2000**, *113*, 8531.
(11) Sakota, K.; Yamamoto, N.; Ohashi, K.; Sekiya, H.; Saeki, M.; Ishiuchi, S.; Sakai, M.; Fujii, M. *Chem. Phys. Lett.* **2001**, *341*, 70.
(12) Le Barbu, K.; Lahmani, F.; Zehnacker-Rentien, A. *J. Phys. Chem. A* **2002**, *106*, 6271.
(13) Matsumoto, Y.; Ebata, T.; Mikami, N. *J. Phys. Chem. B* **2002**, *106*, 5591.
(14) Sakota, K.; Yamamoto, N.; Ohashi, K.; Saeki, M.; Ishiuchi, S.; Sakai, M.; Fujii, M.; Sekiya, H. *Chem. Phys.* **2002**, *283*, 209.
(15) Nibu, Y.; Okabe, C.; Shimada, H. *J. Phys. Chem. A* **2003**, *107*, 1945.
(16) Cho, S. H.; Huh, H.; Kim, H. M.; Kim, N. J.; Kim, S. K. *J. Chem. Phys.* **2005**, *122*, 34305.
(17) Ebata, T.; Hashimoto, T.; Ito, T.; Inokuchi, Y.; Altunsu, F.; Brutschy, B.; Tarakeshwar, P. *Phys. Chem. Chem. Phys.* **2006**, *8*, 4783.
(18) Tanner, C.; Manca, C.; Leutwyler, S. *Science* **2003**, *302*, 1736.
(19) Manca, C.; Tanner, C.; Coussan, S.; Bach, A.; Leutwyler, S. *J. Chem. Phys.* **2004**, *121*, 2578.
(20) Manca, C.; Tanner, C.; Leutwyler, S. *Int. Rev. Phys. Chem.* **2005**, *24*, 457.
(21) Tanner, C.; Thut, M.; Steinlin, A.; Manca, C.; Leutwyler, S. *J. Phys. Chem. A* **2006**, *110*, 1758.
(22) Furche, F.; Ahlrichs, R. *J. Chem. Phys.* **2002**, *117*, 7433.
(23) Ahlrichs, R.; Bär, M.; Häser, M.; Horn, H.; Kölmel, C. *Chem. Phys. Lett* **1989**, *162*, 165. For the current version, see http://www.turbomole.de.
(24) *CPMD*; IBM Corp, MPI für Festkörperforschung: Stuttgart, Germany, 1997−2001.
(25) Rappoport, D.; Furche, F. *J. Chem. Phys.* **2005**, *122*, 064105.
(26) Cai, Z.-L.; Tozer, D. J.; Reimers, J. R. *J. Chem. Phys.* **2000**, *113*, 7084.
(27) Cai, Z.-L.; Reimers, J. R. *J. Chem. Phys.* **2000**, *112*, 527.
(28) Aquino, A. J. A.; Lischka, H.; Hättig, C. *J. Phys. Chem. A* **2005**, *109*, 3201.
(29) Marian, C. M. *J. Chem. Phys.* **2005**, *122*, 104314.
(30) Improta, R.; Santoro, F. *J. Phys. Chem. A* **2005**, *109*, 10058.
(31) Georgieva, I.; Trendafilova, N.; Aquino, A.; Lischka, H. *J. Phys. Chem. A* **2005**, *109*, 11860.
(32) Cai, Z.-L.; Reimers, J. *J. Phys. Chem. A* **2002**, *106*, 8769.
(33) Cai, Z.-L.; Reimers, J. *J. Phys. Chem. A* **2005**, *109*, 1576.
(34) Cai, Z.-L.; Reimers, J. *J. Phys. Chem. A* **2007**, *111*, 954.
(35) Georgieva, I.; Trendafilova, N.; Aquino, A.; Lischka, H. *J. Phys. Chem. A* **2007**, *111*, 127.
(36) Kyrychenko, A.; Waluk, J. *J. Phys. Chem. A* **2006**, *110*, 11958.
(37) Chiba, M.; Tsuneda, T.; Hirao, K. *J. Chem. Phys.* **2006**, *124*, 144106.
(38) Jacquemin, D.; Perpete, E. A.; Scalmani, G.; Frisch, M. J.; Assfeld, X.; Ciofini, I.; Adamo, C. *J. Chem. Phys.* **2006**, *125*, 164324.
(39) Preat, J.; Jacquemin, D.; Wathelet, V.; Andre, J.-M.; Perpete, E. *J. Phys. Chem. A* **2006**, *110*, 8144–8150.
(40) Frisch, M. J. Trucks, G. W.; Schlegel, H. B.; Scuseria, G. E.; Robb, M. A.; Cheeseman, J. R.; Montgomery, J. A., Jr. Vreven, T.; Kudin, K. N.; Burant, J. C.; Millam, J. M.; Iyengar, S. S.; Tomasi, J.; Barone, V.; Mennucci, B.; Cossi, M.; Scalmani, G.; Rega, N.; Petersson, G. A.; Nakatsuji, H.; Hada, M.; Ehara, M.; Toyota, K.; Fukuda, R.; Hasegawa, J.; Ishida, M.; Nakajima, T.; Honda, Y.; Kitao, O.; Nakai, H.; Klene, M.; Li, X.; Knox, J. E.; Hratchian, H. P.; Cross, J. B.; Bakken, V.; Adamo, C.; Jaramillo, J.; Gomperts, R.; Stratmann, R. E.; Yazyev, O.; Austin, A. J.; Cammi, R.; Pomelli, C.; Ochterski, J. W.; Ayala, P. Y.; Morokuma, K.; Voth, G. A.; Salvador, P.; Dannenberg, J. J.; Zakrzewski, V. G.; Dapprich, S.; Daniels, A. D.; Strain, M. C.; Farkas, O.; Malick, D. K.; Rabuck, A. D.; Raghavachari, K.; Foresman, J. B.; Ortiz, J. V.; Cui, Q.; Baboul, A. G.; Clifford, S.; Cioslowski, J.; Stefanov, B. B.; Liu, G.; Liashenko, A.; Piskorz, P.; Komaromi, I.; Martin, R. L.; Fox, D. J.; Keith, T.; Al-Laham, M. A.; Peng, C. Y.; Nanayakkara, A.; Challacombe, M.; Gill, P. M. W.; Johnson, B.; Chen, W.; Wong, M. W.; Gonzalez, C.; Pople, J. A. *Gaussian 03*, revision C.02; Gaussian, Inc.: Wallingford, CT, 2004.
(41) Neugebauer, J.; Louwerse, M. J.; Baerends, E. J.; Wesolowski, T. A. *J. Chem. Phys.* **2005**, *122*, 094115.
(42) Satta, M.; Sanna, N.; Giardini, A.; Speranza, M. *J. Chem. Phys.* **2006**, *125*, 094101.
(43) Lahmani, F.; Douhal, A.; Breheret, E.; Zehnacker-Rentien, A. *Chem. Phys. Lett.* **1994**, *220*, 235.
(44) Bach, A.; Leutwyler, S. *Chem. Phys. Lett.* **1999**, *299*, 381.
(45) Bach, A.; Coussan, S.; Müller, A.; Leutwyler, S. *J. Chem. Phys.* **2000**, *112*, 1192.
(46) Coussan, S.; Bach, A.; Leutwyler, S. *J. Phys. Chem. A* **2000**, *104*, 9864.
(47) Coussan, S.; Manca, C.; Tanner, C.; Bach, A.; Leutwyler, S. *J. Chem. Phys.* **2003**, *119*, 3774.
(48) Bach, A.; Leutwyler, S. *J. Chem. Phys.* **2000**, *112*, 560.
(49) Thut, M.; Manca, C.; Leutwyler, S. *J. Chem. Phys.* **2008**, *128*, 24304.
(50) Becke, A. D. *J. Chem. Phys.* **1993**, *98*, 1053.
(51) Vosko, S.; Wilk, L.; Nusair, M. *Can. J. Phys.* **1980**, *58*, 1200.
(52) Thut, M.; Steinlin, A.; Leutwyler, S. **2008**, in preparation.

JP801044X